Available online at www.sciencedirect.com
ScienceDirect
Continental Shelf Research 27 (2007) 2066–2078
CONTINENTAL SHELF RESEARCH
www.elsevier.com/locate/csr

Aliphatic hydrocarbon concentrations in short sediment cores from the southern Okinawa Trough: Implications for lipid deposition in a complex environment

Woei-Lih Jeng*

Institute of Oceanography, National Taiwan University, Taipei, Taiwan, ROC

Received 8 August 2006; received in revised form 18 April 2007; accepted 7 May 2007
Available online 18 May 2007

Abstract

Seven short sediment cores from the southern Okinawa Trough were collected and analyzed for the aliphatic hydrocarbon concentrations by capillary gas chromatography to explore the deposition of hydrocarbons to this area. For all cores studied, ratios of Σhydrocarbons/TOC, ($nC_{27}+nC_{29}+nC_{31}$)/TOC, terrigenous/aquatic, and diploptene/ΣC_{25-33} *n*-alkanes fluctuated around a mean value with coefficients of variation ranging from 9.0% to 19.7%, 4.9% to 20.0%, 27.3% to 129%, and 3.8% to 163%, respectively. For the $nC_{31}/(nC_{27}+nC_{29}+nC_{31})$ ratio, only station 21 showed fluctuation. Moreover, the carbon preference indexes in the C_{25}–C_{33} *n*-alkane range also exhibited fluctuating values with coefficients of variation of 1.9–14.4%. These results indicate that concentrations of hydrocarbon inputs to the sampling sites vary with time; this may result from complex current flow and sediment transport, leading to variable lipid deposition. In addition, significant correlation between diploptene (hop-22(29)-ene) and higher plant *n*-alkanes was found for cores 21, 42 and 46, indicating that diploptene was predominantly from higher plant sources. However, no correlation between diploptene and higher plant *n*-alkanes was found for cores 20, 36, 43 and 44; autochthonous sources of diploptene in these cores were quite probable.

1. Introduction

Observations from sediment traps show that the sediment fluxes to the southern Okinawa Trough (SOT) are much higher than those in other marginal seas and display great temporal and spatial variability (Hsu et al., 2004). High sedimentation rates are located approximately in the lower trough, deeper than 1000 m (range from 0.25 to 0.52 cm yr^{-1} estimated from the excess ^{210}Pb profiles of cores), while low sedimentation rates are generally in the upper trough, shallower than 1000 m (Chung and Chang, 1995). Based on results from a site (24°48.24′N, 122°30.00′E) of ODP Leg 195 in the SOT, the sedimentation rate has always been high, reaching 325 cm kyr^{-1} (0.325 cm yr^{-1}) since the late Holocene (ODP, 2001). Therefore, the SOT is apparently an area of focused sedimentation along the path of the Kuroshio Current (KC). Furthermore, the lower slope (>1000 m) sediments consist almost entirely of silty mud, while the upper slope (<1000 m) sediments are composed of sand with little mud (Chen et al., 1995).

*Tel.: +886 2 23636040x301; fax: +886 2 23626092.
E-mail address: wljeng@oc.ntu.edu.tw

0278-4343/$ - see front matter © 2007 Elsevier Ltd. All rights reserved.
doi:10.1016/j.csr.2007.05.004

Transport processes of particulate matter in the SOT have been studied in the KEEP (Kuroshio Edge Exchange Processes) program (Wong et al., 2000). From isotopic evidence, Kao et al. (2003) conclude that a major fraction of the sedimentary organic matter in the SOT may originate from the inner shelf of the East China Sea (ECS). Twenty-three surface sediments from the SOT have been shown to receive the highest plant wax *n*-alkane contribution among the coastal marine areas surrounding Taiwan; lateral particle transport from the southern ECS shelf and river runoff from the east Taiwan coast are considered to be the major contributors (Jeng et al., 2003).

The lipid inputs by suspended sediment transport to the SOT derive from three sources (Jeng et al., 2003). One is from the northwest by an alongshore flow just off northern Taiwan. Another is from the nearest river, Lanyang River (LR). The other is from south—the KC carries other river runoffs from eastern Taiwan to the SOT.

Marine sediments may preserve a record of past or on-going environmental processes and components, both natural and human induced. Records in marine sediment can provide information about past biological, chemical and physical oceanographic conditions. As to chemistry, important parameters may include mineral content, major elements, trace elements, total organic carbon (TOC), stable isotope geochemistry, specific organic pollutants, biochemical markers, etc. Organic geochemical data can be used to estimate the total mass of certain compounds in the bottom sediment, to interpret downcore environmental changes as indicated by the abundance and distribution of some compounds present in cores, etc. Because of their stability in the natural environment, aliphatic hydrocarbons are selected and used as a measure for indicating possible change of lipids in sediment cores, which would reflect changes in lipid concentration during sedimentation. The objective of this study was to use the variations of parameters derived from aliphatic hydrocarbon concentrations in 7 short sediment cores collected from the SOT for inferring the condition of lipid deposition in this area.

2. Experimental

In the present study, 7 short sediment cores were collected from the SOT using a box corer on board R/V *Ocean Researcher I* on cruise ORI-417 (April 24–May 1, 1995). Sampling stations are given in Fig. 1. Water depths for stations 20, 21, 36, 42, 43, 44 and 46 are 1096, 1115, 542, 805, 1360, 1465 and 1665 m, respectively. All sub-cores were kept frozen (−20 °C) until analyzed. Cores 20, 42, 43, 44 and 46, respectively, had core lengths of 23, 24, 16, 23.2 and 26.5 cm; each core was sectioned at 4-cm intervals. Cores 21 and 36 had core lengths of 12.5 and 9.5 cm and were sectioned at 2-cm intervals with the last sections of 4.5 and 3.5 cm, respectively. Every section was freeze dried.

Following the addition of an internal standard (n-$C_{24}D_{50}$), the dried sediment was extracted with a mixture of dichloromethane and methanol (1:1, v/v) for 24 h in a Soxhlet apparatus. The lipid extract was then saponified by reflux for 3 h with 0.5 N KOH solution in methanol. The non-saponifiable lipids were isolated by hexane extraction four times and concentrated by solvent evaporation under a N_2 gas stream. The aliphatic hydrocarbon fraction was isolated from the neutral lipids by silica gel (deactivated with 5% H_2O) column chromatography using hexanes.

For GC analysis, an HP 5890A gas chromatograph equipped with a split/splitless injector and a flame ionization detector (FID) was used. Separation of aliphatic hydrocarbons was achieved by an SPB-1 capillary column (30 m × 0.25 mm i.d. × 0.25 μm). Oven temperature programming was 45–90 °C at 15 °C min^{-1} and 90–270 °C at 3 °C min^{-1} for analyzing aliphatic hydrocarbons. Identification was made with co-injection of authentic standards and gas chromatography–mass spectrometry (GC–MS). The GC–MS analyses were performed with an HP 6890 GC (HP-1MS crosslinked methyl siloxane column, 30 m × 0.25 mm i.d. × 0.25 μm) interfaced directly to an HP 5973 quadrupole mass selective detector (electron ionization, electron energy 70 eV, scanned from 50 to 550 Da).

An SGE (Australia) OCI-5 cool on-column injector was also fitted in the gas chromatograph for obtaining the best quantification. GC peak areas of all hydrocarbons and the internal standard were obtained using an electronic integrator (Chromatopac C-R6A, Shimadzu, Japan). Each hydrocarbon concentration was determined using the internal standard. Based on 8 replicate analyses, the analytical imprecision (expressed as the percent coefficient of variation) of hydrocarbon abundances was calculated to be 2–8%.

TOC was quantified with a Fison NA1500 element analyzer. Carbonate carbon was removed

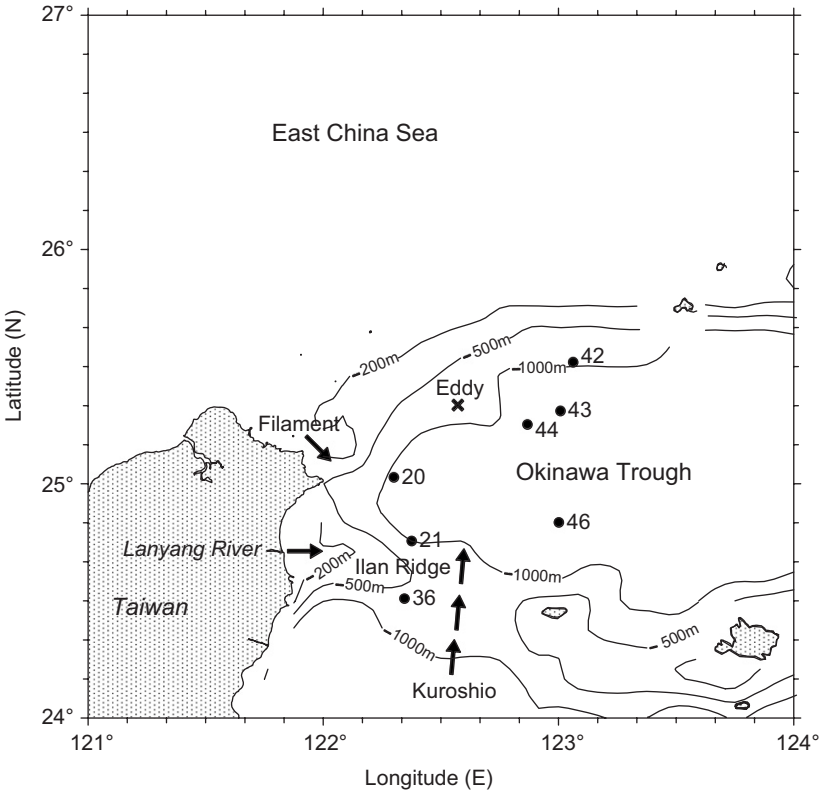

Fig. 1. Sampling locations in the southern Okinawa Trough.

by adding a few drops of 1 N HCl solution to the sediment (<0.5 g) and drying it at 50 °C in an oven. The de-carbonated sample was combusted at 1050 °C in the analyzer, and CO_2 produced was determined with a TCD detector. The relative imprecision for TOC analysis was better than 2.5% ($n = 9$).

3. Results and discussion

Before discussing the lipid data, it is important to briefly describe the flow condition in the SOT. Referring to Fig. 1, the dominant ocean current in the SOT is the KC, which flows approximately northward along the east coast of Taiwan. Its subsurface water shoals up off the northeast coast of Taiwan, and the main stream turns northeastward along the ECS continental slope. However, part of the KC water intrudes on the shelf forming a branch current, termed the Kuroshio Branch Current (KBC). On the western side of the KBC, a cyclonic eddy is generated over the shelf-slope. Seasonal changes in the KC path, partial or extensive intrusion of the KC onto the shelf, and seasonal existence of the eddy can affect the deposition of sedimentary lipids (Liu et al., 1998; Tang et al., 1999). To the northwest of the study area, a southeastward filament (a small alongshore flow) occasionally appears somewhere between the eddy and northern Taiwan (Chern et al., 1990). The flow may transport sediment from the southern ECS shelf to the SOT during its existence. Sediment contribution from the nearby LR from the west is the third source. The annual sediment discharge of the river amounts to ca. 8.0 Mt yr^{-1} (Water Resources Bureau, 1998). The sediment discharge from this river runoff varies over time (Hsu et al., 2004; Lee et al., 2004). For instance, the major transport of river sediment to the sea reaches maximums when high rainfalls cause the river to flood especially during the landfall of typhoons.

A representative GC trace for SOT sediments is shown in Fig. 2, and all hydrocarbon concentrations and related parameters are given in Table 1. In all sediments, higher molecular weight (HMW, $>C_{23}$) *n*-alkanes strongly outweighed lower molecular weight (LMW, $<C_{23}$) ones with strong odd-to-even preference in the HMW range, suggesting a

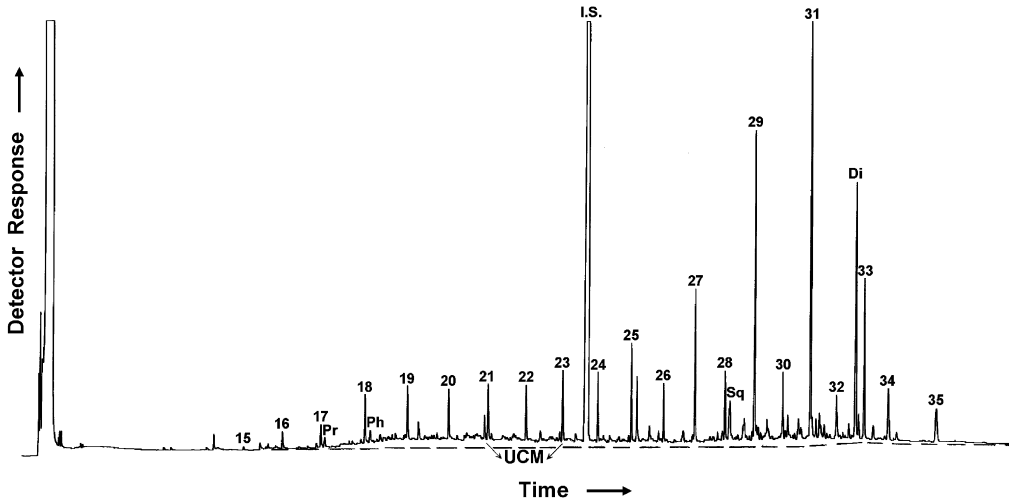

Fig. 2. GC traces of aliphatic hydrocarbons from station 46 (12–16 cm). Numbers above peaks indicate carbon chain lengths. Pr = pristane, Ph = phytane, Sq = Squalene, Di = diploptene, UCM = unresolved complex mixtures.

Table 1
Hydrocarbon concentrations (ng g^{-1}) and related parameters

Compound	Core 20 (0–4 cm)	Core 20 (4–8 cm)	Core 20 (8–12 cm)	Core 20 (12–16 cm)	Core 20 (16–20 cm)	Core 20 (20–23 cm)	Core 21 (0–2 cm)
nC_{15}	—	—	—	—	—	—	119
nC_{16}	10.6	—	—	4.57	—	—	104
nC_{17}	32.4	2.68	22.5	36.9	—	4.99	222
Pristane	13.8	1.34	9.14	11.4	—	—	290
nC_{18}	28.9	21.5	48.5	55.9	5.00	32.2	116
Phytane	10.4	6.45	16.5	20.0	—	8.32	39.5
nC_{19}	28.9	28.3	37.5	51.4	18.2	52.2	84.5
nC_{20}	25.0	25.2	22.5	44.9	28.2	56.3	90.4
nC_{21}	42.7	37.0	32.0	64.7	45.7	64.7	95.2
nC_{22}	51.8	38.6	34.0	62.4	52.2	60.1	130
nC_{23}	109	74.6	78.9	128	118	105	168
nC_{24}	69.1	71.6	59.8	97.8	101	94.0	109
nC_{25}	204	137	155	225	226	190	169
nC_{26}	94.0	69.7	73.9	108	110	93.1	112
nC_{27}	367	252	286	406	420	312	232
nC_{28}	129	93.6	98.1	139	147	114	126
Squalene	132	28.3	74.5	89.2	29.1	38.5	186
nC_{29}	691	565	574	773	805	679	418
nC_{30}	124	99.7	99.7	138	150	143	171
nC_{31}	819	638	658	910	947	699	538
nC_{32}	13.4	74.8	68.3	92.5	94.8	66.7	96.2
Diplop.	42.0	235	13.6	24.5	24.2	17.9	433
nC_{33}	365	288	301	404	427	377	270
nC_{34}	20.8	18.1	17.5	23.6	24.8	43.5	36.7
nC_{35}	101	91.9	84.2	111	130	123	168
UCM[a]	1690	671	373	1240	450	15000	4970
TOC[b]	0.56	0.57	0.47	0.50	0.61	0.54	0.68
ΣHC	3520	2900	2870	4020	3900	3370	4520
ΣHC/TOC[c]	6290	5090	6110	8040	6390	6240	6650
Terr/TOC[d]	3350	2550	3230	4180	3560	3130	1750
TAR[e]	30.6	47.0	25.3	23.7	119	29.6	2.79
nC_{31}/Terr[f]	0.436	0.438	0.433	0.436	0.436	0.414	0.453

Table 1 (*continued*)

Compound	Core 20 (0–4 cm)	Core 20 (4–8 cm)	Core 20 (8–12 cm)	Core 20 (12–16 cm)	Core 20 (16–20 cm)	Core 20 (20–23 cm)	Core 21 (0–2 cm)
CPI[g]	6.06	4.94	5.23	5.07	5.03	4.66	2.81
Di/ΣC_{25-33}[h]	0.017	0.13	0.0069	0.0090	0.0086	0.0079	0.27
Di/TOC[i]	75.0	412	28.9	49.0	39.7	33.1	637
Compound	Core 21 (2–4 cm)	Core 21 (4–6 cm)	Core 21 (6–8 cm)	Core 21 (8–12.5 cm)	Core 36 (0–2 cm)	Core 36 (2–4 cm)	Core 36 (4–6 cm)
NC_{15}	198	—	5.28	—	—	—	—
NC_{16}	146	15.8	41.1	—	17.6	—	27.3
NC_{17}	271	94.6	130	7.55	50.9	34.1	88.4
Pristane	343	108	146	18.7	29.2	16.5	46.2
NC_{18}	149	111	104	19.8	43.8	60.0	88.6
Phytane	61.7	42.2	39.8	8.47	15.8	22.6	30.7
NC_{19}	122	119	91.4	27.2	34.2	47.4	52.9
NC_{20}	125	141	97.8	40.9	32.6	37.7	37.5
NC_{21}	105	108	88.2	52.8	40.1	42.0	42.8
NC_{22}	91.8	95.8	71.2	69.7	40.9	42.8	43.9
NC_{23}	126	131	103	79.0	76.7	89.6	91.8
NC_{24}	129	123	102	88.5	45.5	68.5	68.9
NC_{25}	167	171	139	108	121	166	165
NC_{26}	117	118	88.7	63.7	63.6	84.2	79.3
NC_{27}	244	243	205	173	235	318	308
NC_{28}	123	138	88.9	73.0	91.1	128	114
Squalene	60.8	62.1	29.8	82.3	101	—	—
NC_{29}	430	469	386	369	502	679	677
NC_{30}	158	156	95.6	92.5	81.7	126	112
NC_{31}	481	573	463	441	693	891	876
NC_{32}	123	126	101	64.8	55.4	88.3	93.9
Diplop.	405	442	373	353	36.5	36.3	31.3
NC_{33}	292	285	249	211	316	417	405
NC_{34}	56.4	32.6	34.5	27.3	18.9	25.7	23.6
NC_{35}	133	137	139	129	80.3	102	101
UCM[a]	1700	7980	6420	3550	—	1270	1570
TOC[b]	0.70	0.70	0.63	0.66	0.37	0.39	0.39
ΣHC	4660	4040	3410	2600	2820	3520	3610
ΣHC/TOC[c]	6660	5770	5410	3940	7620	9030	9260
Terr/TOC[d]	1650	1840	1670	1490	3860	4840	4770
TAR[e]	1.95	6.02	4.65	28.3	16.8	23.2	13.2
NC_{31}/Terr[f]	0.416	0.446	0.439	0.449	0.485	0.472	0.471
CPI[g]	2.64	2.84	3.28	3.73	5.76	5.23	5.47
Di/ΣC_{25-33}[h]	0.25	0.25	0.26	0.27	0.020	0.015	0.013
Di/TOC[i]	579	631	592	535	98.6	93.1	80.3
Compound	Core 36 (6–9.5 cm)	Core 42 (0–4 cm)	Core 42 (4–8 cm)	Core 42 (8–12 cm)	Core 42 (12–16 cm)	Core 42 (16–20 cm)	Core 42 (20–24 cm)
NC_{15}	—	8.58	—	—	—	—	—
NC_{16}	—	24.4	6.59	—	—	—	—
NC_{17}	31.3	50.7	61.3	—	8.09	—	7.33
Pristane	15.0	34.3	37.1	—	6.15	—	3.66
NC_{18}	63.9	41.8	89.8	8.15	33.2	—	33.6
Phytane	22.6	14.9	31.1	—	12.2	—	11.3
nC_{19}	46.6	28.9	63.9	26.0	40.3	10.4	44.3
nC_{20}	34.9	28.4	49.1	38.2	40.4	24.0	44.8
nC_{21}	41.8	32.7	57.1	54.1	55.7	43.1	56.0
nC_{22}	43.9	55.3	52.5	58.6	57.6	55.0	58.9
nC_{23}	89.7	92.0	82.2	95.1	98.9	97.6	100

Table 1 (*continued*)

Compound	Core 36 (6–9.5 cm)	Core 42 (0–4 cm)	Core 42 (4–8 cm)	Core 42 (8–12 cm)	Core 42 (12–16 cm)	Core 42 (16–20 cm)	Core 42 (20–24 cm)
nC_{24}	68.0	55.5	70.6	80.2	81.1	77.3	80.7
nC_{25}	163	58.4	124	135	154	149	159
nC_{26}	82.4	33.1	72.7	80.0	88.6	84.8	90.9
nC_{27}	311	81.6	211	225	269	259	284
nC_{28}	117	32.5	91.0	96.5	111	106	143
Squalene	5.69	65.5	94.4	24.5	65.4	70.6	113
nC_{29}	689	154	432	444	536	511	564
nC_{30}	115	38.7	101	105	122	130	127
nC_{31}	899	197	487	510	636	594	679
nC_{32}	86.1	24.4	82.3	87.5	99.6	92.1	82.3
Diplop.	26.2	32.4	90.4	90.1	108	88.4	93.9
nC_{33}	418	90.5	233	247	304	291	331
nC_{34}	24.9	1.88	17.0	19.3	22.3	20.2	28.3
nC_{35}	106	33.4	71.1	77.6	94.8	87.4	98.1
UCM[a]	966	—	1380	1860	1860	1560	828
TOC[b]	0.37	0.31	0.65	0.68	0.67	0.66	0.67
ΣHC	3500	1310	2710	2500	3040	2790	3230
ΣHC/TOC[c]	9460	4230	4170	3680	4540	4230	4820
Terr/TOC[d]	5130	1400	1740	1730	2150	2070	2280
TAR[e]	24.4	4.91	9.03	45.3	29.8	131	29.6
nC_{31}/Terr[f]	0.473	0.455	0.431	0.433	0.441	0.435	0.445
CPI[g]	5.56	3.82	3.83	3.75	4.03	3.93	4.07
Di/ΣC_{25-33}[h]	0.011	0.056	0.061	0.058	0.057	0.049	0.047
Di/TOC[i]	70.8	105	139	133	161	134	140

Compound	Core 43 (0–4 cm)	Core 43 (4–8 cm)	Core 43 (8–12 cm)	Core 43 (12–16 cm)	Core 44 (0–4 cm)	Core 44 (4–8 cm)	Core 44 (8–12 cm)
nC_{15}	—	—	—	—	—	—	—
nC_{16}	—	14.1	—	—	20.8	—	18.7
nC_{17}	7.88	64.6	3.35	7.28	84.0	—	78.1
Pristane	11.3	37.9	5.40	5.15	81.7	—	43.1
nC_{18}	27.7	95.9	26.9	27.8	68.9	11.6	94.7
Phytane	9.93	33.2	10.2	10.4	25.7	—	33.0
nC_{19}	39.7	73.8	40.9	41.2	63.0	32.2	78.2
nC_{20}	45.1	64.5	46.9	42.6	64.2	41.8	72.3
nC_{21}	62.5	63.6	60.3	54.7	80.7	65.9	83.0
nC_{22}	89.8	59.0	58.1	55.2	112	79.0	82.6
nC_{23}	108	78.8	76.9	74.2	130	116	130
nC_{24}	59.4	67.4	65.7	64.8	74.0	84.3	97.5
nC_{25}	96.0	98.4	95.5	95.5	137	170	212
nC_{26}	58.8	62.3	59.7	59.4	81.1	90.6	113
nC_{27}	153	157	153	155	208	297	387
nC_{28}	64.8	65.4	63.6	64.3	105	117	154
Squalene	138	—	—	—	192	96.8	67.4
nC_{29}	288	291	282	288	378	612	782
nC_{30}	97.1	73.2	62.2	72.8	122	115	160
nC_{31}	384	413	377	380	491	742	898
nC_{32}	39.9	69.5	61.0	55.2	71.8	105	120
Diplop.	182	172	105	128	303	236	149
nC_{33}	173	184	172	173	243	309	398
nC_{34}	15.1	15.1	12.1	10.9	36.1	19.5	37.0
nC_{35}	71.8	67.7	62.0	62.3	112	87.3	121
UCM[a]	—	2100	1120	1690	3210	2330	2480
TOC[b]	0.56	0.63	0.62	0.61	0.74	0.72	0.75
ΣHC	2220	2320	1900	1930	3290	3430	4410
ΣHC/TOC[c]	3960	3680	3060	3160	4450	4760	5880

Table 1 (*continued*)

Compound	Core 43 (0–4 cm)	Core 43 (4–8 cm)	Core 43 (8–12 cm)	Core 43 (12–16 cm)	Core 44 (0–4 cm)	Core 44 (4–8 cm)	Core 44 (8–12 cm)
Terr/TOC[d]	1470	1370	1310	1350	1460	2290	2760
TAR[e]	17.3	6.22	18.4	17.0	7.33	51.3	13.2
nC_{31}/Terr[f]	0.465	0.480	0.464	0.462	0.456	0.449	0.434
CPI[g]	3.69	3.69	3.82	3.81	3.34	4.46	4.37
Di/ΣC_{25-33}[h]	0.17	0.15	0.097	0.12	0.21	0.11	0.056
Di/TOC[i]	325	273	169	210	409	328	199

Compound	Core 44 (12–16 cm)	Core 44 (16–20 cm)	Core 44 (20–23.2 cm)	Core 46 (0–4 cm)	Core 46 (4–8 cm)	Core 46 (8–12 cm)	Core 46 (12–16 cm)
nC_{15}	—	—	—	—	7.81	—	—
nC_{16}	—	—	19.4	9.92	52.0	—	2.11
nC_{17}	34.9	—	80.2	58.7	129	—	22.8
Pristane	22.9	—	40.7	60.4	80.9	—	13.6
nC_{18}	70.0	—	105	53.4	109	2.11	49.5
Phytane	24.5	—	31.4	20.9	36.5	—	18.1
nC_{19}	64.9	—	78.5	56.2	71.2	10.8	49.3
nC_{20}	62.9	21.7	67.5	61.3	59.7	21.4	47.9
nC_{21}	76.1	50.9	78.2	73.0	64.6	39.1	56.4
nC_{22}	79.8	68.7	85.7	73.9	63.0	49.5	57.0
nC_{23}	125	116	126	98.8	87.7	73.2	76.5
nC_{24}	92.1	87.7	94.2	67.7	74.5	64.4	66.1
nC_{25}	190	187	180	123	109	101	97.5
nC_{26}	102	99.4	94.8	75.2	65.3	64.3	58.3
nC_{27}	340	337	318	183	172	170	158
nC_{28}	138	134	128	84.0	73.5	74.7	63.2
Squalene	198	27.6	74.0	430	380	78.7	41.9
nC_{29}	676	678	645	335	322	340	314
nC_{30}	143	137	130	86.7	82.5	79.3	68.4
nC_{31}	795	816	805	444	424	449	407
nC_{32}	112	116	107	52.0	52.0	76.5	65.6
Diplop.	101	109	64.3	533	325	403	323
nC_{33}	374	387	368	216	203	194	185
nC_{34}	22.8	24.3	22.9	19.2	14.6	13.2	12.1
nC_{35}	110	115	109	90.0	86.6	81.6	73.7
UCM[a]	3200	1610	3100	—	670	1330	973
TOC[b]	0.70	0.70	0.69	0.68	0.63	0.64	0.61
ΣHC	3950	3510	3850	3310	3150	2390	2330
ΣHC/TOC[c]	5640	5010	5580	4870	5000	3730	3820
Terr/TOC[d]	2590	2620	2560	1410	1460	1500	1440
TAR[e]	18.1	—	11.1	8.37	4.41	88.8	12.2
nC_{31}/Terr[f]	0.439	0.446	0.455	0.462	0.462	0.468	0.463
CPI[g]	4.32	4.45	4.49	3.83	3.91	3.78	3.98
Di/ΣC_{25-33}[h]	0.043	0.045	0.028	0.41	0.26	0.32	0.28
Di/TOC[i]	144	156	93.2	784	516	630	530

Compound	Core 46 (16–20 cm)	Core 46 (20–24 cm)	Core 46 (24–26.5 cm)
nC_{15}	—	—	—
nC_{16}	—	—	—
nC_{17}	38.4	9.27	2.88
Pristane	25.8	4.63	1.44
nC_{18}	64.5	33.8	22.9
Phytane	24.1	12.2	8.33
nC_{19}	54.4	42.4	41.6
nC_{20}	45.3	44.9	54.0
nC_{21}	54.0	55.7	67.1

Table 1 (*continued*)

Compound	Core 46 (16–20 cm)	Core 46 (20–24 cm)	Core 46 (24–26.5 cm)
nC_{22}	51.4	56.5	62.8
nC_{23}	72.1	74.6	77.2
nC_{24}	65.1	64.2	66.1
nC_{25}	97.3	96.8	93.2
nC_{26}	53.7	59.0	53.8
nC_{27}	165	157	149
nC_{28}	61.5	69.6	60.1
Squalene	43.0	126	42.7
nC_{29}	340	308	293
nC_{30}	72.8	65.8	65.0
nC_{31}	463	425	392
nC_{32}	79.5	59.9	68.2
Diplop.	430	253	306
nC_{33}	203	180	170
nC_{34}	11.4	13.0	11.6
nC_{35}	76.9	63.5	66.3
UCM[a]	1070	1910	2740
TOC[b]	0.63	0.58	0.63
ΣHC	2590	2270	2180
ΣHC/TOC[c]	4110	3910	3460
Terr/TOC[d]	1540	1530	1320
TAR[e]	10.4	17.2	18.8
nC_{31}/Terr[f]	0.478	0.478	0.470
CPI[g]	4.18	4.02	3.87
Di/ΣC_{25-33}[h]	0.34	0.22	0.28
Di/TOC[i]	683	436	486

[a]UCM = unresolved complex mixtures.
[b]TOC in unit of gC $(100\,g)^{-1}$.
[c]In unit of 10^{-7} g $(gC)^{-1}$.
[d]Terr/TOC = $(nC_{27}+nC_{29}+nC_{31})$/TOC, in unit of 10^{-7} g $(gC)^{-1}$.
[e]TAR = terrigenous/aquatic ratio = $(nC_{27}+nC_{29}+nC_{31})/(nC_{15}+nC_{17}+nC_{19})$.
[f]nC_{31}/Terr = $nC_{31}/(nC_{27}+nC_{29}+nC_{31})$.
[g]CPI = carbon preference index = $\frac{1}{2}\left(\frac{nC25+nC27+nC29+nC31+nC33}{nC24+nC26+nC28+nC30+nC32}+\frac{nC25+nC27+nC29+nC31+nC33}{nC26+nC28+nC30+nC32+nC34}\right)$.
[h]Di/ΣC_{25-33} = diploptene/$(nC_{25}+nC_{27}+nC_{29}+nC_{31}+nC_{33})$.
[i]Di/TOC = diploptene/TOC, in unit of 10^{-7} g $(gC)^{-1}$.

predominant contribution from higher plant sources (Rieley et al., 1991; Hedges and Prahl, 1993) although shorter-chain *n*-alkanes were more prone to degradation than longer-chain ones (Meyers et al., 1984; Gagosian and Peltzer, 1986). The odd-carbon predominance in the C_{25}–C_{33} range was strongest among the coastal marine sediments surrounding Taiwan. In addition, most samples showed a small baseline elevation, the so-called "unresolved complex mixtures" (UCM). UCM is known to consist of cyclic and branched alkanes and to resist microbial degradation more effectively than *n*-alkanes, and thus has a greater tendency to remain in the environment after *n*-alkanes have degraded (Gough and Rowland, 1990; Bouloubassi and Saliot, 1993). This does not necessarily reflect the content of degraded petroleum in the sediments since in some cases concentrations of UCM $<10\,\mu g\,g^{-1}$ are common in coastal marine environments far from petrogenic hydrocarbon sources (Matsumoto, 1983; Tolosa et al., 1996). Only one core section (bottom of station 20) gave a UCM value $>10\,\mu g\,g^{-1}$. In addition, *n*-alkanes were prominent, indicating little weathering.

For comparing all sections in a core, total hydrocarbon concentrations were normalized to TOC for eliminating the grain size effect. As indicated in Table 2, cores 20, 21, 36, 42, 43, 44 and 46, respectively, gave the following averages and standard deviations: $6360 \pm 951 \times 10^{-7}$ g $(gC)^{-1}$

Table 2
Averages and coefficients of variance for parameters

Core	Parameter	Average ± 1s.d.	(%) Coefficient of variance (C.V.)
20	ΣHC/TOC[a]	6360 ± 951	15.0
	$(nC_{27}+nC_{29}+nC_{31})$/TOC[b]	3333 ± 536	16.1
	TAR	45.9 ± 36.8	80.2
	$nC_{31}/(nC_{27}+nC_{29}+nC_{31})$	0.432 ± 0.009	2.1
	CPI	5.17 ± 0.48	9.3
	$Di/\Sigma C_{25-33}$	0.030 ± 0.049	163
21	ΣHC/TOC	5686 ± 1119	19.7
	$(nC_{27}+nC_{29}+nC_{31})$/TOC	1680 ± 130	7.7
	TAR	8.74 ± 11.0	126
	$nC_{31}/(nC_{27}+nC_{29}+nC_{31})$	0.441 ± 0.015	3.4
	CPI	3.06 ± 0.44	14.4
	$Di/\Sigma C_{25-33}$	0.26 ± 0.01	3.8
36	ΣHC/TOC	8843 ± 834	9.4
	$(nC_{27}+nC_{29}+nC_{31})$/TOC	4650 ± 549	11.8
	TAR	19.4 ± 5.3	27.3
	$nC_{31}/(nC_{27}+nC_{29}+nC_{31})$	0.475 ± 0.007	1.5
	CPI	5.51 ± 0.22	4.0
	$Di/\Sigma C_{25-33}$	0.015 ± 0.004	26.7
42	ΣHC/TOC	4278 ± 384	9.0
	$(nC_{27}+nC_{29}+nC_{31})$/TOC	1895 ± 329	17.4
	TAR	41.6 ± 46.3	111
	$nC_{31}/(nC_{27}+nC_{29}+nC_{31})$	0.440 ± 0.009	2.0
	CPI	3.91 ± 0.13	3.3
	$Di/\Sigma C_{25-33}$	0.055 ± 0.005	9.1
43	ΣHC/TOC	3465 ± 428	12.4
	$(nC_{27}+nC_{29}+nC_{31})$/TOC	1375 ± 68	4.9
	TAR	14.7 ± 5.7	38.8
	$nC_{31}/(nC_{27}+nC_{29}+nC_{31})$	0.468 ± 0.008	1.7
	CPI	3.75 ± 0.07	1.9
	$Di/\Sigma C_{25-33}$	0.13 ± 0.03	23.1
44	ΣHC/TOC	5220 ± 564	10.8
	$(nC_{27}+nC_{29}+nC_{31})$/TOC	2380 ± 476	20.0
	TAR	20.2 ± 17.8	88.1
	$nC_{31}/(nC_{27}+nC_{29}+nC_{31})$	0.447 ± 0.009	2.0
	CPI	4.24 ± 0.44	10.4
	$Di/\Sigma C_{25-33}$	0.082 ± 0.069	84.1
46	ΣHC/TOC	4129 ± 586	14.2
	$(nC_{27}+nC_{29}+nC_{31})$/TOC	1457 ± 77	5.3
	TAR	22.9 ± 29.5	129
	$nC_{31}/(nC_{27}+nC_{29}+nC_{31})$	0.469 ± 0.007	1.5
	CPI	3.94 ± 0.13	3.3
	$Di/\Sigma C_{25-33}$	0.30 ± 0.06	20.0

[a,b]In unit of 10^{-7} g $(gC)^{-1}$.

(C.V. = 15.0%), $5686 \pm 1119 \times 10^{-7}$g $(gC)^{-1}$ (C.V. = 19.7%), $8843 \pm 834 \times 10^{-7}$g $(gC)^{-1}$ (C.V. = 9.4%), $4278 \pm 384 \times 10^{-7}$g $(gC)^{-1}$ (C.V. = 9.0%), $3465 \pm 428 \times 10^{-7}$g $(gC)^{-1}$ (C.V. = 12.4%), $5220 \pm 564 \times 10^{-7}$g $(gC)^{-1}$ (C.V. = 10.8%) and $4129 \pm 586 \times 10^{-7}$g $(gC)^{-1}$ (C.V. = 14.2%). Total aliphatic hydrocarbon concentrations normalized to TOC (ΣHC/TOC) among cores spanned a wide range. Referring to Fig. 1, high averages of ΣHC/TOC were found at stations 20, 21 and 36, closer to the shore; low averages were found at stations 42, 43, 44 and 46, farther from the shore. This result reflects that

stations close to land receive more contribution from higher plants since HMW *n*-alkanes are the predominant components in the sediments. Hydrocarbon concentration profiles in a core can be affected by hydrocarbon degradation after burial and hydrocarbon input from the water column to sediment. Compared with other compound classes, aliphatic hydrocarbons especially *n*-alkanes are relatively unreactive and unlikely to be affected by any mechanism that would be selective for alternating homologs in the sequence (Hedges and Prahl, 1993). This means that aliphatic hydrocarbon concentrations are expected to remain virtually constant with core depth as long as input concentrations do not change. To obtain a high precision for lipid analysis, on-column injection in GC has been used routinely in this lab for the last 15 years. The overall measurement imprecision (i.e., reproducibility—from the weighing of sediment samples to the final GC determination) is expressed as the percent coefficient of variation (%C.V. or 1 standard deviation expressed as percentage of the mean concentration). Analytical imprecision varied nonlinearly over a range of analyte concentrations and generally gave a low % C.V. for high analyte concentrations (e.g. hundreds of $ng\,g^{-1}$) and a high %C.V. for low analyte concentrations (e.g., multi-$ng\,g^{-1}$). If hydrocarbon inputs to the sediment remain constant over time, total hydrocarbon concentrations in a core are estimated to have an overall measurement imprecision of 8% at most, considering the worst case. In the present result, great variations (C.V. range 9.0–19.7%) in the ratios of ΣHC/TOC for the 7 cores exceeded the estimated imprecision (8.4% calculated from hydrocarbon imprecision 8% and TOC imprecision 2.5%), suggesting that hydrocarbon inputs to each core varied with time. It is noted that station 21 closest to the LR exhibited a relatively high C.V. of 19.7%, partially attributable to episodic high sediment discharges of the river such as heavy rainfall after typhoons make landfall (Hsu et al., 2004; Lee et al., 2004). Relatively high C.V.s for ΣHC/TOC values were found for stations 20 (15%) and 21 (19.7), and low C.V.s were found for stations 36 (9.4%), 42 (9.0%), 43 (12.4%), 44 (10.8) and 46 (14.2%) (Table 2). This result suggests that stations 20 and 21 received irregular inputs from the LR and filament and that station 36 did not, probably because of the northward flow of the KC.

Higher plant *n*-alkanes were the predominant components in the sediments from the SOT; they were at the concentration of hundreds of $ng\,g^{-1}$ with a low measurement imprecision of 2%. To correct for the grain size effect, $(nC_{27}+nC_{29}+nC_{31})$/TOC was used to estimate the input of higher plant *n*-alkanes to SOT sediments. In general, $(nC_{27}+nC_{29}+nC_{31})$/TOC ratios in Table 2 were higher at stations close to shore than those away from shore with the exception of station 21. The low ratio at station 21 is considered to be influenced by the direct input from the LR, which is known to contain relatively low proportions of terrigenous sources (Jeng and Huh, 2006). Compared with the calculated imprecision of $(nC_{27}+nC_{29}+nC_{31})$/TOC (3.2%), the 7 cores exhibited great variations (C.V. range 4.9–20.0%), attributable to varied inputs from higher plant sources. Stations 20, 42 and 44 with relatively high C.V.s of 16.1%, 17.4% and 20.0%, respectively, are located in the north of the study area and approximately along the path where the KC turns. This could be explained as a result of episodic inputs of HMW *n*-alkanes from the filament and LR to the SOT as well as deposition of these alkanes along the path of the KC.

The ratio of terrigenous-to-aquatic *n*-alkanes were estimated as terrigenous/aquatic ratio (TAR) $= (nC_{27}+nC_{29}+nC_{31})/(nC_{15}+nC_{17}+nC_{19})$. This ratio is valuable for determining changes in relative contributions of organic matter from land and aquatic flora although it may over-represent the absolute amounts from terrigenous sources (Meyers, 1997). This ratio was adopted in the present study to estimate the relative contribution of terrigenous and marine sources to the cored sediments. Stations 20 and 42 showed comparatively high TAR values (45.9 and 41.6, respectively) among the 7 cores, which could be caused by input of sediment with high TAR values from the ECS shelf known to contain high proportions of relict sediments (Niino and Emery, 1961; Chen et al., 1995). The relict sediments presumably have high TAR ratios based on the fact that aquatic *n*-alkanes degrade faster than terrigenous *n*-alkanes. Based on the calculated imprecision of TAR, 8.2% ($nC_{27}+nC_{29}+nC_{31}$ imprecision 2% and $nC_{15}+nC_{17}+nC_{19}$ imprecision 8%), far greater variations of TAR (C.V. range 27.3–129%) were found for all cores, probably attributing to varied inputs of terrigenous and marine hydrocarbon sources. Again a minimum C.V. was found for station 36, indicating that the input of hydrocarbon sources was relatively stable.

In the HMW region, the C_{27} and C_{29} *n*-alkanes are diagnostic of waxes from trees and shrubs, and the *n*-C_{31} alkane is diagnostic of grass waxes. The $nC_{31}/(nC_{27}+nC_{29}+nC_{31})$ ratio was employed to see if any difference existed among the 7 cores. As listed in Table 2, low ratios were found at stations 20 (0.432), 21 (0.441), 42 (0.440), and 44 (0.447); high ratios were found at stations 36 (0.475), 43 (0.468) and 46 (0.469). The results might reveal that the sediments with high ratios may receive more contribution from grass waxes than from tree and shrub waxes. Alternatively, the low ratios may be caused by the input from the LR, which has *n*-alkane distribution maximizing at nC_{29} (7 out of 9 sediments, Jeng and Huh, 2006). It is quite likely that suspended sediment with low $nC_{31}/(nC_{27}+nC_{29}+nC_{31})$ from the river enters the sea, merges into the KC, and flows along the continental slope of the ECS, resulting in those stations with low ratios (Fig. 1). All stations but station 21 showed constant $nC_{31}/(nC_{27}+nC_{29}+nC_{31})$ ratios in a core, judging from the result that the C.V. of each core was smaller than the calculated imprecision of 2.8 (measurement imprecisions of C_{27}, C_{29} and C_{31}, 2%). The result appears to mean that only station 21 is influenced. Note that the $nC_{31}/(nC_{27}+nC_{29}+nC_{31})$ ratio is solely sensitive in responding to the great change of C_{31} *n*-alkane since it is the most abundant component of the aliphatic hydrocarbons.

Owing to the CPIs of terrestrial higher plant waxes yielding high values, usually ~5–10, higher CPI values found in sediment or soil show greater contribution from vascular plants (Rieley et al., 1991; Hedges and Prahl, 1993); CPI values close to unity are thought to indicate greater input from microorganisms, recycled organic matter, and/or petroleum (Bray and Evans, 1961; Farrington and Tripp, 1977; Kennicutt et al., 1987). In the present study, the average CPIs ranged from 3.06 (core 21) to 5.51 (core 36) (Table 2). This reflects that most marine sediments are relatively free of contamination of petrogenic hydrocarbons based on CPI values <3 indicating oiled sediments (Farrington and Tripp, 1977) and no known oil pollution in the area for a long period before sampling. It should be noted that lower CPI values of 2.81, 2.64 and 2.84 (Table 1) were found in the upper 3 sections of station 21; this could be partially attributed to a greater influence from the nearby LR, which exported suspended matter derived from relatively old carbon—the bedrock of argillite-slate and meta-sandstone—due to massive road construction in 1975–1980 (Kao and Liu, 1996; Jeng and Kao, 2002). On the other hand, the lower 2 sections exhibited higher CPI values of 3.28 and 3.73 (Table 2), presumably representing the values before humans disturbed the river.

Referring to Table 2, variations (mean $\pm$ 1 s.d.) of CPIs in the 7 cores are as follows: core 20, 5.17 ± 0.48 (C.V. = 9.3%); core 21, 3.06 ± 0.44 (C.V. = 14.4%); core 36, 5.51 ± 0.22 (C.V. = 4.0%); core 42, 3.91 ± 0.13 (C.V. = 3.3%); core 43, 3.75 ± 0.07 (C.V. = 1.9%); core 44, 4.24 ± 0.44 (C.V. = 10.4%); 3.94 ± 0.13 (C.V. = 3.3%). It should be mentioned that core 21 showed the largest C.V. for CPI, which could be partially attributed to receiving more input of lower CPIs from the LR, resulting in large change in CPI. All 7 cores studied were relatively short (9.5–26.5 cm) and were collected mainly from the Trough with high sedimentation. Little or no diagenetic change in the concentration of aliphatic hydrocarbons is expected. Moreover, the CPI is a diagenetically insensitive ratio because it is based on the relative abundances of chemically similar compounds within a limited molecular weight range (Hedges and Prahl, 1993). CPI's of all cores fluctuated with the core depth. This result indicates that *n*-alkane inputs to the study area vary with time. C.V.s for CPI are relatively high for stations 20 (9.3%), 21 (14.4%), and 44 (10.4%) and comparatively low for stations 36 (4.0%), 42 (3.3%), 43 (1.9%) and 46 (3.3%). It appears that stations with high C.V.s are located close to the LR and filament and hence are under the direct influence of them. It is interesting that station 21 showed the highest C.V. due to the direct input from the LR exporting old hydrocarbons.

Diploptene (hop-22(29)-ene) is derived from terrestrial higher plants and is also formed by bacteria (Rohmer et al., 1984). Prahl (1985) observes an offshore increase in the ratio of diploptene to combined C_{25}, C_{27}, C_{29}, C_{31}, C_{33} plant wax *n*-alkanes ($Di/\Sigma C_{25-33}$) in sediments throughout the southern Washington continental shelf and slope region, and the ratio is used to compare marine sediments and soils (Prahl et al., 1992). As displayed in Table 2, high average ratios of $Di/\Sigma C_{25-33}$ were found for cores 21 (0.26 ± 0.01, C.V. = 3.8%), 43 (0.13 ± 0.03, C.V. = 23.1%) and 46 (0.30 ± 0.06, C.V. = 20.0%), and low average ratios were found for cores 20 (0.030 ± 0.049, C.V. = 163%), 36 (0.015 ± 0.004, C.V. = 26.7%), 42 (0.055 ± 0.005, C.V. = 9.1%), and 44 ($0.082\pm$

0.069, C.V. = 84.1%). Compared with the average $Di/\Sigma C_{25-33}$ ratio (0.16 ± 0.05, C.V. = 32%) (calculated from Jeng and Huh, 2004) of 9 surface sediments from the ECS covering a relatively larger area (4° latitude × 1.5° longitude), the present $Di/\Sigma C_{25-33}$ ratios have a wider range for a relatively smaller area (1° latitude × 50′ longitude). The result may suggest that the input of diploptene and higher plant *n*-alkanes to the study area is more complex than that to the ECS. Moreover, a comparison with the nearby LR with high sediment discharge is worthwhile. The average $Di/\Sigma C_{25-33}$ ratio of 7 surface sediments from this river is 0.30 ± 0.14 (C.V. = 47%) (calculated from Jeng and Huh, 2006), which is comparable to those of cores 21, 43 and 46. The river samples cover a large area with different environments, but for a core site each section is supposedly deposited in the same sedimentary environment. Therefore, the C.V.s of these three cores are considered fairly large, implying variable inputs. Besides, the average $Di/\Sigma C_{25-33}$ ratio of river samples is closer to those of cores 21 and 46 (which and river mouth lie on a straight line), likely implying that the river might be a significant contributor to the two stations. The large differences in $Di/\Sigma C_{25-33}$ ratios between cores can be attributed to (1) varied input of diploptene from higher plant sources and (2) possible input of bacterial diploptene to the study area based on the fact that submarine hydrothermal activities have been observed (Lee et al., 1998; Hsu et al., 2003). If higher plants are the sole source of diploptene, a strong correlation between diploptene and terrestrial higher plant *n*-alkanes has been demonstrated (Prahl et al., 1992). For instance, positive correlations between diploptene and higher plant *n*-alkanes were found for cores 21 ($\Sigma C_{25-33} = -215 + 4.39$ Di, $r = 0.97$), 42 ($\Sigma C_{25-33} = 1.02 + 18.6$ Di, $r = 0.94$) and 46 ($\Sigma C_{25-33} = 980 + 0.628$ Di, $r = 0.82$). However, no such correlation was found for cores 20, 36, 43 and 44; contributions of diploptene mainly from bacteria were unlikely because series of long-chain odd-predominant *n*-alkanes were typically absent (Kolattukudy, 1976) and because CPI values of the 4 cores were high (Table 2). Venkatesan (1988) reviews reports of the occurrence of diploptene in coastal marine sediments on a very broad geographic basis and concludes that this compound derives largely from autochthonous sources. It is thought that diploptene in the 4 cores might be generated in situ analogous to that of perylene (Silliman et al., 2000). If this is the case, an increasing trend for the diploptene/TOC ratio would be expected. However, no such trend was observed for the 4 cores probably because they were too short for diagenetically produced diploptene to be clearly observed.

In summary, the 7 sediment cores have been found to show great variations in ΣHC/TOC, $(nC_{27} + nC_{29} + nC_{31})$/TOC, TAR and $Di/\Sigma C_{25-33}$ ratios as well as CPI values. The results can be attributed to hydrocarbon inputs to the study area fluctuating over time; this may be caused by complex current flow and sediment transport, resulting in a complicated environment for lipid deposition. This is supported by the observation from sediment traps that sediment fluxes to the SOT display great temporal and spatial variability (Hsu et al., 2004).

Acknowledgments

My thanks go to the captain, crew and technicians of the R/V *Ocean Researcher I* for help with sediment collection. I am grateful to Prof. Philip A Meyers (University of Michigan) and one anonymous reviewer for constructive comments and suggestions. This study was financially supported by the National Science Council, Republic of China, Grant no. NSC93-2611-M-002-016.

References

Bouloubassi, I., Saliot, A., 1993. Investigation of anthropogenic and natural organic inputs in estuarine sediments using hydrocarbon markers (NAH, LAB, PAH). Oceanologica Acta 16, 145–161.

Bray, E.E., Evans, E.D., 1961. Distribution of *n*-paraffins as a clue to recognition of source beds. Geochimca et Cosmochimica Acta 22, 2–15.

Chen, M.P., Lin, K.L., Huang, C.K., 1995. Sedimentary structure and texture of surficial sediment off northeastern Taiwan. Ti-Chih (ROC) 15, 15–47 (in Chinese with English abstract).

Chern, C.S., Wang, J., Wang, D.P., 1990. The exchange of Kuroshio and East China Sea shelf water. Journal of Geophysical Research 95, 16017–16023.

Chung, Y., Chang, W.C., 1995. Pb-210 fluxes and sedimentation rates on the lower continental slope between Taiwan and the South Okinawa Trough. Continental Shelf Research 15, 149–164.

Farrington, J.W., Tripp, B.W., 1977. Hydrocarbons in western North Atlantic surface sediments. Geochimica et Cosmochimica Acta 41, 1627–1641.

Gagosian, R.B., Peltzer, E.T., 1986. The importance of atmospheric input of terrestrial organic material to deep sea sediments. Organic Geochemistry 10, 661–669.

Gough, M.A., Rowland, S.J., 1990. Characterization of unresolved complex mixtures of hydrocarbons in petroleum. Nature 344, 648–650.

Hedges, J.I., Prahl, F.G., 1993. Early diagenesis: consequences for applications of molecular biomarkers. In: Engel, M.H., Macko, S.A. (Eds.), Organic Geochemistry: Principles and Applications. Plenum Press, New York, pp. 237–253.

Hsu, S.C., Lin, F.J., Jeng, W.L., Chung, Y.C., Shaw, L.M., 2003. Hydrothermal signatures in the southern Okinawa Trough detected by the sequential extraction of settling particles. Marine Chemistry 84, 49–66.

Hsu, S.C., Lin, F.J., Jeng, W.L., Chung, Y.C., Shaw, L.M., Hung, K.W., 2004. Observed sediment fluxes in the southwesternmost Okinawa Trough enhanced by episodic events: flood runoff from Taiwan rivers and large earthquakes. Deep-Sea Research I 51, 979–997.

Jeng, W.L., Kao, S.J., 2002. Lipids in suspended matter from the human-disturbed Lanyang River, northeastern Taiwan. Environmental Geology 43, 138–144.

Jeng, W.L., Huh, C.A., 2004. Lipids in suspended matter and sediments from the East China Sea Shelf. Organic Geochemistry 35, 647–660.

Jeng, W.L., Huh, C.A., 2006. A comparison of sedimentary aliphatic hydrocarbon distribution between the southern Okinawa Trough and a nearby river with high sediment discharge. Estuarine, Coastal and Shelf Science 66, 217–224.

Jeng, W.L., Lin, S., Kao, S.J., 2003. Distribution of terrigenous lipids in marine sediments off northeastern Taiwan. Deep-Sea Research II 50, 1179–1201.

Kao, S.J., Liu, K.K., 1996. Particulate organic carbon export from a subtropical mountainous river (Lanyang Hsi) in Taiwan. Limnology and Oceanography 41, 1749–1757.

Kao, S.J., Lin, F.J., Liu, K.K., 2003. Organic carbon and nitrogen contents and their isotopic compositions in surficial sediments from the East China Sea shelf and the southern Okinawa Trough. Deep-Sea Research II 50, 1203–1217.

Kennicutt II, M.C., Barker, C., Brooks, J.M., DeFreitas, D.A., Zhu, G.H., 1987. Selected organic matter source indicators in the Orinoco, Nile and Changjiang deltas. Organic Geochemistry 11, 41–51.

Kolattukudy, P.E., 1976. Chemistry and Biochemistry of Natural Waxes. Elsevier, Amsterdam.

Lee, C.S., Chung, S.L., SPOT Members, 1998. Southernmost part of the Okinawa Trough (SPOT): an active extension/collision/subduction area. EOS Transaction of American Geophysical Union 79, W109.

Lee, S.Y., Huh, C.A., Su, C.C., You, C.F., 2004. Sedimentation in the Southern Okinawa Trough: enhanced particle scavenging and teleconnection between the Equatorial Pacific and western Pacific margins. Deep-Sea Research I 51, 1769–1780.

Liu, C.T., Cheng, S.P., Chuang, W.S., Yang, Y., Lee, T.N., Johns, W.E., Li, H.W., 1998. Mean structure and transport of Taiwan Current (Kuroshio). Acta Oceanographica Taiwanica 36, 159–176.

Matsumoto, G., 1983. Comparative study on organic constituents in polluted and unpolluted inland aquatic environments—V. Organic carbons and hydrocarbons in sediments. Water Research 17, 823–830.

Meyers, P.A., 1997. Organic geochemical proxies of paleoceanographic, paleolimnologic, and paleoclimatic processes. Organic Geochemistry 27, 213–250.

Meyers, P.A., Leenheer, M.J., Eadie, B.J., Maule, S.J., 1984. Organic geochemistry of suspended and settling particulate matter in Lake Michigan. Geochimica et Cosmochimica Acta 48, 443–452.

Niino, H., Emery, K.O., 1961. Sediments of shallow portions of East China Sea and South China Sea. Geological Society of America Bulletin 72, 731–762.

ODP, 2001. Seafloor Observatories and the Kuroshio Current. Ocean Drilling Program, Leg 195 Preliminary Report. Available at: 〈http://www-odp.tamu.edu/publications/prelim/195_prel/195toc.html〉.

Prahl, F.G., 1985. Chemical evidence of differential particle dispersal in the southern Washington coastal environment. Geochimica et Cosmochimica Acta 49, 2533–2539.

Prahl, F.G., Hayes, J.M., Xie, T.M., 1992. Diploptene: an indicator of terrigenous organic carbon in Washington coastal sediments. Limnology and Oceanography 37, 1290–1300.

Rieley, G., Collier, R.J., Jones, D.M., Eglinton, G., 1991. The biogeochemistry of Ellesmere Lake, UK—I: source correlation of leaf wax inputs to the sedimentary lipid record. Organic Geochemistry 17, 901–912.

Rohmer, M., Bouvier-Nave, P., Ourisson, G., 1984. Distribution of hopanoid triterpenes in prokaryotes. Journal of General Microbiology 130, 1137–1150.

Silliman, J.E., Meyers, P.A., Ostrom, P.H., Ostrom, N.E., Eadie, B.J., 2000. Insights into the origin of perylene from isotopic analyses of sediments from Saanich Inlet, British Columbia. Organic Geochemistry 31, 1133–1142.

Tang, T.Y., Hsueh, Y., Yang, Y.J., Ma, J.C., 1999. Continental slope flow northeast of Taiwan. Journal of Physical Oceanography 29, 1353–1362.

Tolosa, I., Bayona, J.M., Albaigés, J., 1996. Aliphatic and polycyclic aromatic hydrocarbons and sulfur/oxygen derivatives in northwestern Mediterranean sediments: spatial and temporal variability, fluxes and budgets. Environmental Science and Technology 30, 2495–2503.

Venkatesan, M.I., 1988. Diploptene in Antarctic sediments. Geochimica et Cosmochimica Acta 52, 217–222.

Water Resources Bureau, 1998. Hydrological Year Book of Taiwan, Republic of China 1997. Ministry of Economic Affairs, Taipei, Taiwan, Republic of China, p. 23.

Wong, G.T.F., Chao, S.Y., Li, Y.H., Shiah, F.K., 2000. The Kuroshio edge exchange processes (KEEP) study—an introduction to hypotheses and highlights. Continental Shelf Research 20, 335–347.